Analytical theory of optical transmission through periodically structured metal films via tunnel-coupled surface polariton modes

Sergey A. Darmanyan,[1] Michel Nevière,[2] and Anatoly V. Zayats[3,*]
[1]*Institute of Spectroscopy, Russian Academy of Sciences, Troitsk, Moscow reg., 142190, Russia*
[2]*Institut Fresnel, Faculté des Sciences et Techniques de Saint Jérome, 13397 Marseille Cedex 20, France*
[3]*School of Mathematics and Physics, International Research Centre for Experimental Physics, The Queen's University of Belfast, Belfast BT7 1NN, United Kingdom*
(Received 13 November 2003; revised manuscript received 20 February 2004; published 13 August 2004)

Analytical calculations of light transmission through and reflection from periodically structured metal films due to tunnel coupling of surface plasmon polariton modes are presented. The influence of the adjacent media has been studied in both symmetric and asymmetric configurations. The transmission spectra have been analyzed in different regimes corresponding to double-resonant and single-resonant tunneling. The electromagnetic field configuration related to the surface polariton Bloch modes of the film has been derived that allows direct estimation of far- and near-field distributions of the reflected and transmitted light. The analytically calculated spectra are in a good agreement with numerical modeling as well as available experimental data. The theory provides a description of optical properties of periodically structured metal films with topography variations and/or dielectric constant modulation.

DOI: 10.1103/PhysRevB.70.075103 PACS number(s): 78.67.−n, 42.25.Fx

I. INTRODUCTION

Optical transmission through and reflection from periodically structured metallic films capable of supporting surface plasmon polaritons (SPPs) attracts continuous attention due to its possible numerous applications and unexpected properties related to the SPP interactions. The ability to control surface polariton behavior on surfaces and thin films is extremely important for modern photonic and optoelectronic technologies.[1,2] Metallic nanostructures have been considered for applications as nanoscale surface plasmon based sensors, wavelength selective optical filters, for the enhancement of nonlinear optical processes, and can lead to the development of passive and active functional components of all-optical photonic circuits.[1–6]

The optical phenomena related to the SPP properties on periodic surface stuctures are resonant absorption, reflection, as well as enhanced transmission. All these phenomena are in one or another way related to the SPP Bloch modes formed on a periodically structured surface. The most interesting and most complex effect is the enhancement or suppression of the optical transmission through periodically nanostructured metal films. After the first experimental observations,[6] theoretical and experimental investigations of the enhanced transmission have addressed the transmission mechanisms through hole and slit structures,[7] the evanescent field coupling between the interfaces of a metal film,[8] the role of the SPP Bloch modes and the near-field effects,[9] the influence of the metal film surroundings,[10] control of the optical transmission via the enhanced nonlinear response of metallic nanostructures,[5] and many others. The transmission enhancement can be observed through metallic films with and without openings in a film.[3,4,11] In addition to waveguiding modes, possible in the case of slits in a metal film,[7] and cylindrical surface plasmons which can contribute to the transmission of holes,[5] tunneling between the states of surface plasmon polariton Bloch modes has been identified as one of the mechanisms of the transmission enhancement which is always present at certain resonant wavelengths.[3,4]

The development of analytical and numerical approaches has allowed us to understand the main principles of the enhanced transmission such as the difference between hole [two-dimensional] and slit [one-dimensional] arrays, the nonnecessity of holes or slits in a film (only one or another kind of periodic modulation is needed, such as topography or dielectric constant variations), the role of the SPP states related to different branches of the Brillouin zones in photon tunneling through a metallic film, etc. Analytical descriptions are beneficial for identification of the transmission mechanisms. They might provide direct dependencies on all parameters of a nanostructure and allow optimization of the transmission in a desirable spectral range. The first analytical attempts to describe the transmission properties of the periodically nanostructured metal films were focused on the establishment of the SPP Bloch mode states participating in the tunneling process,[3] followed by the studies of the optically induced transmission of a metal film placed in the symmetric environment.[4] The electromagnetic mode structure of a periodically modulated surface near the even SPP band gaps has been investigated since only these SPP states participate in the optical processes involving normally incident photons. It was shown that the states of the related Brillouin zones can be coupled to photons in the neighboring medium and the tunneling between these states determine the transmission enhancement at normal incidence.[3]

In this paper we consider optical transmission via surface polariton modes taking into account the interaction between the SPP modes on the opposite film interfaces, i.e., the exact film SPP modes. This allows derivation of the analytical expressions for transmission and reflection of the periodically structured metal film surrounded by different dielectric media and analysis of the transmission mechanisms in different

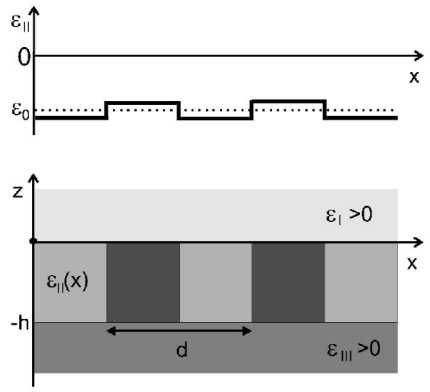

FIG. 1. Geometry of a periodically structured metal film.

regimes. The exact knowledge of the electromagnetic mode structure is used to study near- and far-field properties of the transmitted light.

II. RESULTS AND DISCUSSION

A. SPP film modes of a periodic structure

Let us consider a metallic film of a finite thickness with periodic modulation of the dielectric properties throughout the film thickness. This can be either topographic modulation due to slits or holes in the film, metal permittivity modulation, or filling of the slits or holes with other material. The film is placed between two generally different dielectric media (Fig. 1). The structure is characterized by the dielectric constants $\varepsilon_I > 0$ for $z > 0$, $\varepsilon_{III} > 0$ for $z < -h$, and ε_{II} for $-h < z < 0$. The dielectric constant ε_{II} is assumed to be periodic in the x direction, i.e., $\varepsilon_{II}(x) = \varepsilon_{II}(x+nd)$, $n = 1, 2...$, and its average value is negative, $<\varepsilon_{II}> = \varepsilon_0 < 0$ (please do not mix ε_0 with the vacuum permittivity). For simplicity we consider the case of the real dielectric functions $\varepsilon_{I,II,III}$.

The structure is illuminated at normal incidence from the medium I and the electromagnetic surface waves can be excited on the structure interfaces due to periodic modulation. In the case of the transverse magnetic wave propagating along the x axis with the wave vector k_x, the electromagnetic field has the following form with both transverse and longitudinal components of the electric field

$$\boldsymbol{E} = (E_x, 0, E_z)e^{ik_x x - i\omega t} + \text{c.c.}, \quad \boldsymbol{H} = (0, H_y, 0)e^{ik_x x - i\omega t} + \text{c.c.} \tag{1}$$

The method of treating the electromagnetic properties of periodic structures is well developed and consists in substitution of the field and dielectric function in the Maxwell equations by their Fourier expansions

$$\boldsymbol{E} = \sum_{n=-\infty}^{\infty} \boldsymbol{E}_n \exp(ingx), \quad \varepsilon_{II} = \sum_{n=-\infty}^{\infty} \varepsilon_n \exp(ingx), \tag{2}$$

where $g = 2\pi/d$ is the vector of the reciprocal lattice related to the periodic structure. After straightforward algebra one arrives to the set of equations for the field amplitudes that are usually studied numerically.[12]

The first band gap in the spectrum of SPPs on a periodically structured surface lies in the nonradiative region, therefore, higher SPP band gaps must be considered for the description of light transmission. We are interested only in the electromagnetic field configuration of the branches of the SPP Bloch modes near the bottom edges of the even band gaps, since only these states have complex (with imaginary part) frequencies and, thus, can interact with normally incident photons.[3] To get analytical expressions for the dispersion law of the film modes and in particular the width and position of the band gap edges as well as the field configurations and amplitudes of the reflected and transmitted waves, we restrict ourselves to the simple case of $\varepsilon_{II}(x) = \varepsilon_0 + 2\varepsilon_1 \cos(gx)$. Here, ε_1 is the first coefficient of the Fourier expansion of ε_{II} [Eq. (2)] that determines the variation of the dielectric function of the metal film. The field configuration near the second band gap can be calculated by truncating the Fourier series for fields, and the electric field in the metallic medium can be sought in the form

$$\boldsymbol{E}_{II} = (\boldsymbol{A} + \boldsymbol{B}\cos gx + \boldsymbol{C}\sin gx)e^{\kappa z}, \tag{3}$$

where $\boldsymbol{A}$, $\boldsymbol{B}$, $\boldsymbol{C}$, and κ are the parameters that should be determined. This is the so-called three-wave approximation which is generalization of the two-wave approximation commonly used in solid state physics for the description of the Bloch states near the first band gap. Being substituted into the Maxwell equations, Eq. (3) leads to the set of six equations for six field amplitudes $A_{x;z}$, $B_{x;z}$, $C_{x;z}$. It is important to note that this set of equations splits into two independent sets for the fields A_x, B_x, C_z and A_z, B_z, C_x. Conditions of solvability of the first set of equations lead to the following expressions for four eigenvalues κ_i:

$$\kappa_{1,2}^2 = \frac{1}{2}\left(g^2 - 2\varepsilon_0 k_0^2 \mp \sqrt{g^4 + 8\alpha_1 \varepsilon_0 k_0^2 (\varepsilon_0 k_0^2 - g^2)}\right)$$
$$\approx \begin{cases} -\varepsilon_0 k_0^2 - 2\alpha_1 \varepsilon_0 k_0^2 (\varepsilon_0 k_0^2 - g^2)/g^2 \\ g^2 - \varepsilon_0 k_0^2 + 2\alpha_1 \varepsilon_0 k_0^2 (\varepsilon_0 k_0^2 - g^2)/g^2 \end{cases}, \tag{4}$$

while the conditions of solvability of the second set gives remaining two eigenvalues

$$\kappa_3^2 = -\varepsilon_0 k_0^2 + \frac{g^2}{1 - 2\alpha_1} \approx -\varepsilon_0 k_0^2 + g^2 + 2\alpha_1 g^2, \tag{5}$$

where $k_0 = \omega/c$ is the light wave vector in vacuum (ω is the light frequency) and $\alpha_1 = \varepsilon_1^2/\varepsilon_0^2$ depends on the metal permittivity variation across the film. Only three of six eigenvalues κ_i are independent since $\kappa_{4,5,6} = -\kappa_{1,2,3}$.

The approximations made in Eqs. (4) and (5) are valid for $\alpha_1 = \varepsilon_1^2/\varepsilon_0^2 \ll 1$, or to be more precise in the case of Eq. (4), when the second term in the square root is much smaller than the first one. This condition can be written as

$$8\varepsilon_1^2 \frac{d^2}{\lambda^2}\left(\frac{d^2}{\lambda^2} - \frac{1}{\varepsilon_0}\right) \approx 8\varepsilon_1^2 \frac{d^4}{\lambda^4} \ll 1. \tag{6}$$

Here, $\lambda = 2\pi/k_0$ is the light wavelength in vacuum. Equation (6) shows that the absolute value of the dielectric constant modulation depth $|\varepsilon_1|$ is more important than the ratio $|\varepsilon_1/\varepsilon_0|$.

Thus, within the chosen three-wave approximation [Eq. (3)], the field in the medium II has the following form:

$$E_x = (A_{1;x} + B_{1;x}\cos gx)e^{\kappa_1 z} + (A_{2;x} + B_{2;x}\cos gx)e^{\kappa_2 z} + C_{3;x}\sin gx e^{\kappa_3 z} + (a_{1;x} + b_{1;x}\cos gx)e^{-\kappa_1(z+h)} + (a_{2;x} + b_{2;x}\cos gx)e^{-\kappa_2(z+h)} + c_{3;x}\sin gx\, e^{-\kappa_3(z+h)},$$

$$E_z = C_{1;z}\sin gx\, e^{\kappa_1 z} + C_{2;z}\sin gx\, e^{\kappa_2 z} + (A_{3;z} + B_{3;z}\cos gx)e^{\kappa_3 z} + c_{1;z}\sin gx\, e^{-\kappa_1(z+h)} + c_{2;z}\sin gx\, e^{-\kappa_2(z+h)} + (a_{3;z} + b_{3;z}\cos gx)e^{-\kappa_3(z+h)}, \quad (7)$$

where the fields of the corresponding eigenmodes are related as

$$A_{1,2;x} = \frac{-\varepsilon_1 k_0^2}{\varepsilon_0 k_0^2 + \kappa_{1,2}^2} B_{1,2;x}, \quad C_{1,2;z} = \frac{g\kappa_{1,2}}{g^2 - \varepsilon_0 k_0^2} B_{1,2;x},$$

$$A_{3;z} = \frac{-\varepsilon_1}{\varepsilon_0} B_{3;z}, \quad C_{3;x} = \frac{\kappa_3}{g}(2\alpha_1 - 1)B_{3;z}. \quad (8)$$

Similar relations hold for the amplitudes a, b, and c with κ_i substituted by $-\kappa_i$.

B. Transmission and reflection coefficients

Light transmission through and reflection from a metal film are determined by the fields in the dielectric media I and III. We take these fields in the form

$$E_x = A_x e^{-ik_I z} + R_x e^{ik_I z} + (B_x\cos gx + C_x\sin gx)e^{-\eta_I z},$$

$$E_z = (B_z\cos gx + C_z\sin gx)e^{-\eta_I z} \quad (9)$$

for $z>0$, where the incident, reflected, and SPP fields are present, and

$$E_x = T_x e^{-ik_{III}(z+h)} + (b_x\cos gx + c_x\sin gx)e^{\eta_{III}(z+h)},$$

$$E_z = (b_z\cos gx + c_z\sin gx)e^{\eta_{III}(z+h)} \quad (10)$$

for $z<-h$, where the transmitted and SPP fields exist. Here,

$$k_{I,III}^2 = \varepsilon_{I,III} k_0^2, \quad \eta_{I,III}^2 = g^2 - \varepsilon_{I,III} k_0^2, \quad (11)$$

$$C_z = -\frac{g}{\eta_I} B_x, \quad C_x = \frac{\eta_I}{g} B_z, \quad c_z = \frac{g}{\eta_{III}} b_x, \quad c_x = -\frac{\eta_{III}}{g} b_z, \quad (12)$$

where A, R, and T are the amplitudes of the incident, reflected, and transmitted waves, respectively.

Upon substitution of expressions (7), (9), and (10) into corresponding boundary conditions, we arrive at two independent sets of equations for the field amplitudes. The set of the boundary conditions for the fields A_x, B_x, and C_z contains the incident amplitude A_x and 18 unknown amplitudes. Using Eqs. (8) and (12) and analogous relations between $a_{1x,2x}, b_{1x,2x}$, and $c_{1z,2z}$, the full system of equations can be reduced to the system of 4 equations defining 4 amplitudes $A_{1x,2x}$ and $a_{1x,2x}$ in terms of the incident field amplitude A_x:

$$\begin{pmatrix} \Psi_1 & \Psi_2 & \Psi_1^* e^{-\kappa_1 h} & \Psi_2^* e^{-\kappa_2 h} \\ \varphi_1 F_1 & \varphi_2 F_2 & \varphi_1 \overline{F}_1 e^{-\kappa_1 h} & \varphi_2 \overline{F}_2 e^{-\kappa_2 h} \\ \psi_1^* e^{-\kappa_1 h} & \psi_2^* e^{-\kappa_2 h} & \psi_1 & \psi_2 \\ \varphi_1 \overline{f}_1 e^{-\kappa_1 h} & \varphi_2 \overline{f}_2 e^{-\kappa_2 h} & \varphi_1 f_1 & \varphi_2 f_2 \end{pmatrix} \begin{pmatrix} A_{1x} \\ A_{2x} \\ a_{1x} \\ a_{2x} \end{pmatrix} = \begin{pmatrix} 2k_I A_x \\ 0 \\ 0 \\ 0 \end{pmatrix}. \quad (13)$$

In writing down Eq. (13) the following notations were introduced:

$$F_{1,2} = \frac{\varepsilon_I}{\eta_I} + \frac{\varepsilon_0\kappa_{1,2}}{g^2 - \varepsilon_0 k_0^2}, \quad \overline{F}_{1,2} = \frac{\varepsilon_I}{\eta_I} - \frac{\varepsilon_0\kappa_{1,2}}{g^2 - \varepsilon_0 k_0^2},$$

$$f_{1,2} = \frac{\varepsilon_{III}}{\eta_{III}} + \frac{\varepsilon_0\kappa_{1,2}}{g^2 - \varepsilon_0 k_0^2}, \quad \overline{f}_{1,2} = \frac{\varepsilon_{III}}{\eta_{III}} - \frac{\varepsilon_0\kappa_{1,2}}{g^2 - \varepsilon_0 k_0^2}, \quad (14)$$

and

$$\Psi_{1,2} = k_I + i\kappa_{1,2}, \quad \psi_{1,2} = k_{III} + i\kappa_{1,2}, \quad \varphi_{1,2} = \kappa_{1,2}^2 + \varepsilon_0 k_0^2. \quad (15)$$

Now it is straightforward to get the expressions for the field amplitudes: $A_{1x,2x} = d_{1,2}/d$ and $a_{1x,2x} = d_{3,4}/d$. Here $d = \det[M]$ is the determinant of the 4×4 matrix defined in the left hand side of Eq. (13) and $d_{1,2,3,4}$ are the determinants of the matrixes obtained from the matrix M by replacing the corresponding column with the column defined in the right hand side of Eq. (13). Using this, one can easily find the transmitted and reflected field amplitudes

$$T_x = (d_1 e^{-\kappa_1 h} + d_2 e^{-\kappa_2 h} + d_3 + d_4)/d,$$

$$R_x = (d_1 + d_2 + d_3 e^{-\kappa_1 h} + d_4 e^{-\kappa_2 h})/d - A_x. \quad (16)$$

The equation $d=0$ defines the dispersion relation of the SPP modes existing on a structured film. In the particular case of a single interface, which is given by limit $h\to\infty$, it reproduces the dispersion relation of the surface electromagnetic mode obtained in Ref. 3, while in the case of $\alpha_1 \to 0$ it gives the dispersion relation of the excitations of a homogeneous film.[13] Equations (16) together with the corresponding expressions for the determinants d and d_i give the solution of the problem of the light transmission through the periodically nanostructured metal film capable of supporting surface plasmon polaritons.

C. Transmission spectra

We have analyzed the transmission spectra of the metallic structures with parameters similar to those studied in the experiments and used for numerical modeling.[7,10,11] In particular, we considered a gold film deposited on a quartz substrate ($\varepsilon_{III}=2.31$). The film was illuminated from the side opposite to the substrate. To model the dielectric function of gold we used the approximation $\varepsilon_0 = 1 - 3\times 10^{-5}(\lambda[\mathrm{nm}])^2$ which is valid in the spectral range $\lambda = 600-1000$ nm. The permittivi-

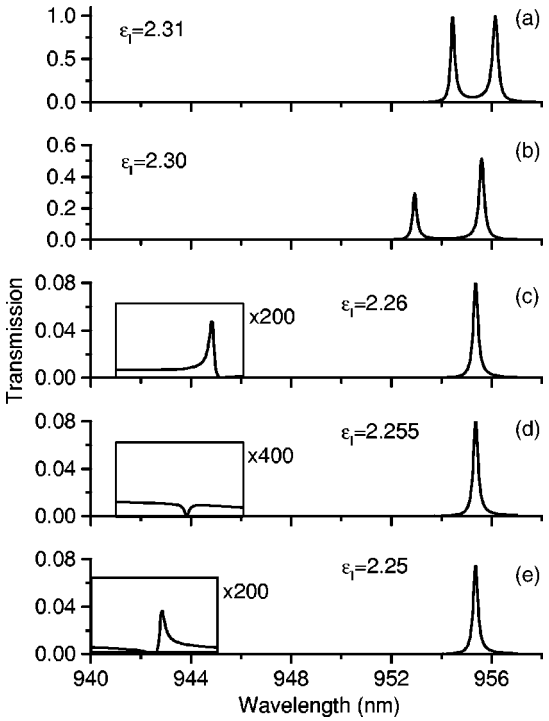

FIG. 2. Intensity transmission spectra of the periodically structured gold film deposited on the quartz substrate ($\varepsilon_{III}=2.31$) for different dielectric constant of the adjacent medium ε_I. The film thickness is 150 nm. Periodicity is $d=600$ nm with 50% duty cycle. Modulation depth is $|\varepsilon_1/\varepsilon_0|=0.1$.

ties of the adjacent medium were varied in the range $\varepsilon_I=1-2.31$ in order to clarify the transmission mechanisms related to degenerate and nondegenerate SPP modes on the film interfaces. Only real part of the dielectric constant of gold was taken into account for simplicity, but the influence of the Ohmic losses will also be discussed. The analytically calculated transmission spectra $t=|T_x/A_x|^2$ obtained using Eq. (16) are similar to the experimentally observed spectra and those given by numerical calculations. The spectral position, shape of spectral bands as well as their behavior with refractive index changes and thickness of the film are described well by the analytical expressions.

The transmission spectra are presented in Figs. 2 and 3 for different dielectric constants of the adjacent medium ε_I. In the case of a symmetric structure (a metal film sandwiched in quartz), the spectrum consists of two peaks of equal amplitudes. The peak wavelengths are very close in the case of the relatively thick film. For smaller film thicknesses these peaks move in opposite directions with the decrease of the thickness, preserving their amplitudes $t=1$. With the increase of the thickness, the transmission peaks shift closer, and transmission becomes smaller. These peaks correspond to the film SPP Bloch modes of the nanostructured metal film. In symmetric surroundings, the SPP modes related to the opposite interfaces are degenerated and the interaction leads to splitting of their frequencies and formation of the film SPP modes with symmetric (low-frequency mode) and antisymmetric (high-frequency mode) distributions of the field in the film. For relatively thick films, the SPP modes are weakly

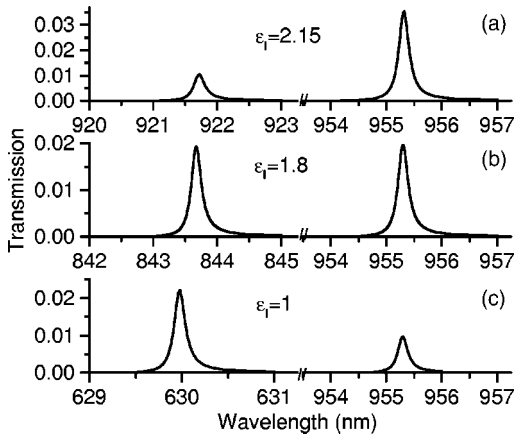

FIG. 3. Intensity transmission spectra of the periodically structured gold film deposited on the quartz substrate for different dielectric constant of the adjacent medium ε_I. The parameters of the structure are the same as in Fig. 2.

interacting and thus shifted only slightly from each other. With the decrease of the thickness they are repulsed further.

The transmission is expected to be $t=1$ in the case of a symmetric structure. This follows from the considerations of the resonant tunneling between the SPP modes on the opposite film interfaces (double-resonant conditions).[3] Irrespectively of the film thickness, the full transfer of the excitation energy occurs through the film if the SPP lifetime is long enough, similarly to the tunneling through a potential barrier via resonant states of quantum wells. However, in the case of very thick films, the decrease in the transmission was observed. This is related to the increase of the interaction time needed to achieve effective tunneling through a thick film. Although the Ohmic losses are absent, the radiative losses due to coupling back to photons reduce the SPP lifetime. If the imaginary part of the dielectric constant of metal is taken into considerations, the amplitude of the peaks drops and they become wider. In the case of a thick film (and thus a weak coupling between SPP modes) the separation between two peaks is very small and this fine structure of the transmission spectra may be very sensitive to the value of the Ohmic losses.[4] If the Ohmic losses are included, this leads to one transmission peak observed which is related to two closely spaced SPP resonances.[11] The decrease of the transmittance in both described earlier situations is related to one or another kind of losses in the system leading to the finite SPP lifetime and therefore, reducing tunneling efficiency. Thus, the use of metals with low Ohmic losses is advantageous for photonic applications of such nanostructures. The temperature dependence of Ohmic losses can be very important for optical applications at low temperatures (including space-based applications) where conventional optical elements have short lifetimes and are difficult to use.

If the symmetry of the structure is broken [Figs. 2(b–e) and 3], the SPP modes are not degenerated but still interact with each other. A short-wavelength mode is related to the interface of the medium with a lower dielectric constant which is varied in the calculations, and shifts to the high frequency range with the decrease of the refractive index. At the same time, the long-wavelength mode related to a quartz

interface is shifted much less since it is influenced only by a weak interaction between the SPP modes. For thinner films, this shift is much more pronounced.

Since in the asymmetric case, due to the difference in the position of SPP resonances on opposite interfaces, the double-resonant tunneling conditions are not satisfied, the transmission becomes smaller in both resonances. In this case, the transmission peaks are related to direct photon tunneling via one of the SPP resonances. Initially, with the decrease of ε_{I} the peak transmittance corresponding to the SPP on the interface in contact with the ε_{I} dielectric is smaller than the other peak. (In the opposite case, with the increase of ε_{I}, a symmetrical picture is observed with the longer-wavelength resonant transmittance decreasing faster.) However, two distinctively different transmission regimes can be identified when the dielectric constant ε_{I} is varied [cf. Figs. 2(b,c) and 2(e), 3. The transition between these two regimes is clearly observed at some value of the dielectric constant [Fig. 2(d)] which depends on the film thickness. For close values of the dielectric constants of surroundings (weakly asymmetric case) the SPP Bloch modes of the interfaces "remember" the symmetry of the film SPP modes. With the increase of the asymmetry, the short-wavelength transmission peak becomes smaller and disappears at some value of the dielectric constant at which the transmission at the SPP wavelength is suppressed compared to the transmission of the unstructured film and reaches zero. The physical reason for this behavior is a crossing of the SPP mode states associated with the two systems of the Bloch modes of surface polaritons on the opposite film interfaces. The decrease in the transmission and its suppression occurs due to the cancellation of the propagative fields associated with these two modes which are radiated with opposite phase to each other.[15] If the Ohmic losses are present, this leads to a significant absorption at this wavelength. With the further increase of the difference in the dielectric constants of surroundings, these SPP modes become separated in energy and the high-frequency transmission peak appears again. However, the shape of the resonance has different symmetry corresponding to the density of states in the Brillouin zone.

Further decrease of the dielectric constant leads to the increase of the short-wavelength peak and the decrease of the long-wavelength transmission until they become equal in the amplitude [Fig. 3(b)], then the high-frequency mode becomes dominating [Fig. 3(c)]. This behavior is determined by the different behavior of the $\kappa_{1,2}$ coefficients that describes spatial extension of the two SPP modes with the dielectric constant change. This leads to different tunneling probabilities related to these modes.

In the case of light incident from the side of a substrate, the transmission coefficient can be calculated by exchanging dielectric constants of the substrate and the superstrate $\varepsilon_{\mathrm{III}} \leftrightarrow \varepsilon_{\mathrm{I}}$. The transmittance ratio in this case is determined by the ratio of corresponding dielectric constants $t_{\mathrm{III}\to\mathrm{I}}/t_{\mathrm{I}\to\mathrm{III}} = \varepsilon_{\mathrm{III}}/\varepsilon_{\mathrm{I}}$. This is a consequence of the fact that the relative transmittance measured as the ratio of the transmitted energy flow (the time averaged Poynting vector) $S_t = (c/8\pi) n_{\mathrm{I,III}} |T|^2$ to the incident energy flow $S_i = (c/8\pi) n_{\mathrm{III,I}} |A|^2$ is equal in both directions. This is valid for the total energy transmitted through the nanostructure. If the structure transmission has, in addition to zero order, also higher transmitted orders which propagate at some angle to the incident light direction, the transmission in the individual orders might not provide reciprocity with respect to the illumination side of the asymmetric nanostructure. Even if the transmission is the same, the reflection and absorption of the asymmetric structure depends on the side which is illuminated.[11]

D. Film electromagnetic modes versus individual surface modes

To analyze the importance of the SPP Bloch modes interaction and formation of the film SPP modes in the case of a film of a finite thickness, it is useful to further simplify the expressions for the transmission and reflection coefficients, that can be achieved for some parameters of the structure but may not hold in every case. According to Eq. (13) the expression for the determinant d can be approximated as

$$\begin{aligned} d \approx \Delta_1\Delta_2 &- e^{-2h\kappa_1}(\varphi_2 F_2 \Psi_1^* - \varphi_1 \overline{F_1}\Psi_2)(\varphi_2 f_2 \psi_1^* - \varphi_1 \overline{f_1}\psi_2) \\ &- e^{-2h\kappa_2}(\varphi_1 F_1 \Psi_2^* - \varphi_2 \overline{F_2}\Psi_1)(\varphi_1 f_1 \psi_2^* - \varphi_2 \overline{f_2}\psi_1) \\ &+ \varphi_1\varphi_2 e^{-h(\kappa_1+\kappa_2)}[(\overline{F_2}\Psi_2 - F_2\Psi_2^*)(\overline{f_1}\psi_1 - f_1\psi_1^*) \\ &+ (\overline{F_1}\Psi_1 - F_1\Psi_1^*)(\overline{f_2}\psi_2 - f_2\psi_2^*)], \end{aligned} \tag{17}$$

where

$$\Delta_1 = \varphi_2 F_2 \Psi_1 - \varphi_1 F_1 \Psi_2, \quad \Delta_2 = \varphi_2 f_2 \psi_1 - \varphi_1 f_1 \psi_2. \tag{18}$$

We have omitted above the small terms proportional to $\exp[-2h(\kappa_1+\kappa_2)]$.

To simplify the expressions for the field amplitudes and dispersion relation, one can note that along with the parameters $\gamma_1 = \exp(-h\kappa_1)$ and $\gamma_2 = \exp(-h\kappa_2)$, that are small for a not very thin film, the relation $\varphi_1 \ll \varphi_2 \simeq g^2$ holds in the case of $|\varepsilon_1| \ll 1$. We also assume that, in spite of $\gamma_1 > \gamma_2$, the inequality $\varphi_1\gamma_1 \ll g^2\gamma_2$ is satisfied. Taking into account that at the resonance either F_2 or f_2 is proportional to φ_1, we neglect in Eq. (17) the terms containing products of small parameters φ_1, F_2, or f_2 and the exponents. Then the expression for the determinant d is reduced to

$$d \approx \Delta_1\Delta_2 - e^{-2h\kappa_2}\varphi_2^2 \overline{F_2}\,\overline{f_2}\Psi_1\psi_1. \tag{19}$$

As was mentioned earlier, the equation $\Delta_i = 0$ defines the dispersion relations of SPPs at an individual interface. An approximate solution to this equation was found in Ref. 3. In the case of a film of a finite thickness, these dispersion relations are slightly modified due to the last term in the right hand side of Eq. (19), which describes interaction between two interface excitations. For a homogeneous (unstructured) film this term plays an important role. Namely, in the case of asymmetric surroundings ($\varepsilon_{\mathrm{I}} \neq \varepsilon_{\mathrm{III}}$) it describes the coupling of the upper SPP mode, related to the interface with the dielectric medium of lower ε, to bulk modes of the dielectric medium of a higher refractive index. At the same time in the symmetric system ($\varepsilon_{\mathrm{I}} = \varepsilon_{\mathrm{III}}$), it describes the difference between symmetric and antisymmetric SPP modes. Nevertheless, for the problem considered here of the optical transmission of the structured film this term can be neglected in the

asymmetric case, since it brings only exponentially small shift [proportional to $\gamma_2^2=\exp(-2h\kappa_2)$] of the resonant frequency. The solutions of the equation $d=0$ that gives the resonant excitation frequencies, are complex valued. In real experiments one can change only the frequency of the incident wave that is real valued. Thus, the condition of $d=0$ as well as $\Delta_i=0$ cannot be reached (the resonance has a finite height and a finite width determined by the losses in the system—in our case, the coupling to the bulk modes—that determine also the imaginary part of the resonant frequency). To solve the problem of the enhanced transmission efficiency one must define the magnitude and the position of $\max(|T_x|)$, that lies in the vicinity of $\min(|d|)$. In turn the $\min(|d|)$ is situated in the vicinity of either $\min(|\Delta_1|)$ that corresponds to the SPP resonance on one of the interfaces, or $\min(|\Delta_2|)$ that corresponds to the SPP resonance on another interface. When the positions of $\min(|\Delta_1|)$ and $\min(|\Delta_2|)$ coincide (or they are very close to each other), the $\min(|d|)$ becomes much deeper and as a consequence the magnitude of the $\max(|T_x|)$ is additionally increased. We refer to this case as a double-resonant one.[3] In Ref.10 it was experimentally and numerically demonstrated, that the transmission enhancement factor through the perforated metal films is much higher in the symmetric case when the dielectric constants of the media surrounding a metal film are the same ($\varepsilon_\mathrm{I}=\varepsilon_\mathrm{III}$). The later condition leads to the relation $\Delta_2=\Delta_1$. As can be inferred from Eq. (19), in this case $d\approx(\Delta_1-\varphi_2\overline{F_2}\Psi_1 e^{-h\kappa_2})(\Delta_1+\varphi_2\overline{F_2}\Psi_1 e^{-h\kappa_2})$, and two solutions of the equation $d=0$ differ by the exponentially small term only. Thus, in this case the double-resonant photon tunneling via these SPP states takes place. It should be noted that in the symmetric case the shift of the resonant frequency is proportional to γ_2 while in the asymmetric case it behaves as γ_2^2.

Having calculated the determinants d_i and keeping only the terms of the lowest order in small parameters, we can find the approximate expression for the amplitude of the transmitted and reflected waves in the form

$$T_x \approx \frac{2k_\mathrm{I}A_x}{d}(\varphi_2F_2D_1e^{-h\kappa_1}-\varphi_1F_1D_2e^{-h\kappa_2}), \tag{20}$$

$$R_x \approx \frac{d_1+d_2}{d}-A_x \approx A_x\left(2k_\mathrm{I}\Delta_2\frac{\varphi_2F_2-\varphi_1F_1}{d}-1\right), \tag{21}$$

where

$$\begin{aligned} D_1 &= \Delta_2+i\varphi_1\overline{f_1}(\kappa_2-\kappa_1)+\psi_1^*(\varphi_1f_1-\varphi_2f_2)\\ &= 2i\kappa_1f_2(\varphi_2-\varphi_1)\approx 2i\kappa_1f_2\varphi_2,\\ D_2 &= \Delta_2+i\varphi_2\overline{f_2}(\kappa_2-\kappa_1)+\psi_2^*(\varphi_1f_1-\varphi_2f_2)\\ &= 2i\kappa_2f_1(\varphi_2-\varphi_1)\approx 2i\kappa_2f_1\varphi_2. \end{aligned} \tag{22}$$

Therefore, the intensity transmission is

$$t=\left|\frac{T_x}{A_x}\right|^2 \approx \frac{16k_1^2\varphi_2^2}{|d|^2}|\kappa_1\varphi_2F_2f_2e^{-h\kappa_1}-\kappa_2\varphi_1F_1f_1e^{-h\kappa_2}|^2. \tag{23}$$

We note that the transmission in the regions close to either the first SPP resonance $\Delta_1=0$ (for which $F_2\sim\varphi_1$) or to the second SPP resonance $\Delta_2=0$ (for which $f_2\sim\varphi_1$) are described by Eqs. (20) and (23) while in the region far from both resonances, this formulae can be simplified, e.g., Eq. (20) is reduced to

$$T_x \approx \frac{4ik_\mathrm{I}A_x\kappa_1\varphi_2^2F_2f_2}{d}e^{-h\kappa_1} \approx \frac{4ik_\mathrm{I}\kappa_1A_x}{\psi_1\Psi_1}e^{-h\kappa_1}. \tag{24}$$

Equation (24) describes the nonresonant transmission through a film and at $\kappa_1=k_0\sqrt{|\varepsilon_0|}$ coincides with the dependence for an unstructured film.

E. Near-field and far-field transmission

Expressions (16) describe the field amplitudes in the far-field region. Knowledge of the near-field is very important for many applications and especially for consideration of nonlinear optical properties of the structure if the nonlinearity of a metal itself or nonlinear material deposited on the metal surface should be taken into account. It is the electromagnetic field enhancement in the near-field region close to a metallic structure that makes possible the observation of the nonlinear optical effects at very low incident light intensities.[5,14]

The analytical approach described earlier permits determination of the near-field amplitudes as well. According to Eq. (10), the total electromagnetic near-field on the interface opposite to the illuminated one, i.e., at $z=-h-0$, is described by $E_x=T_x+b_x\cos gx$ and $E_z=c_z\sin gx$, with $c_z=gb_x/\eta_\mathrm{III}$. The fields proportional to c_x and b_z cannot be excited with normally incident light, as was discussed earlier, and are omitted from the near-field description. However, these fields can be significant at oblique illumination.[15]

Using Eq. (8) and the respective boundary conditions, the following expressions for the coefficient b_x can be derived

$$\begin{aligned} b_x &= -\frac{1}{\varepsilon_1k_0^2}[\varphi_1(a_{1x}+A_{1x}e^{-\kappa_1h})+\varphi_2(a_{2x}+A_{2x}e^{-\kappa_2h})]\\ &\simeq \frac{4k_\mathrm{I}A_x\varphi_2^2\varphi_1\varepsilon_0}{\varepsilon_1k_0^2(g^2-\varepsilon_0k_0^2)d}[\kappa_2F_1\psi_1e^{-h\kappa_2}-\kappa_1F_2\psi_2e^{-h\kappa_1}]. \end{aligned} \tag{25}$$

Thus, in contrast to the far-field region, the near-field of the transmitted light has the nonzero component E_z normal to the interface. This effect is responsible for significant polarization conversion observed in the near-field. The electric field normal to the surface is related to the nonradiative part of the SPP Bloch wave and cannot be detected in the far-field, where the polarization of the transmitted light is the same as the incident light polarization. This polarization effect is important for scanning near-field microscopy of nanostructured metals since the interpretation of the near-field images depends on the efficiency of coupling of different polarization

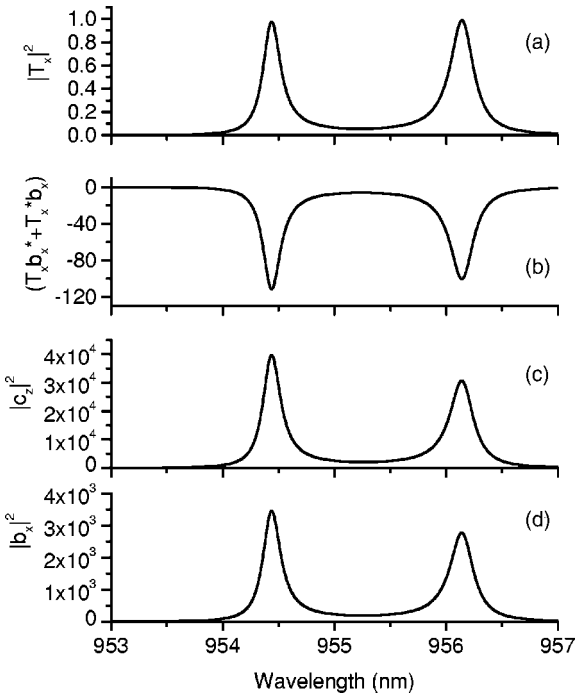

FIG. 4. Spectral dependencies of the coefficients in Eq. (26) determining the near-field intensity across the surface: (a) $|T_x|^2$, (b) $|T_x b_x^* + T_x^* b_x|$, (c) $|c_z|^2$, and (d) $|b_x|^2$. The parameters of the structure are the same as in Fig. 2(a).

components of the field over a surface to a fiber tip and the polarization dependent electromagnetic field enhancement at the tip apex. Polarization properties of the transmitted light in the near-field should also be taken into account when considering nonlinear optical interactions which can exhibit profound polarization dependencies due to the symmetry properties of the second- and/or third-order nonlinear susceptibilities.

The evanescent field component E_z exhibits a resonant behavior with the incident light frequency similar to T_x. However, it is proportional to $\sin(gx)$, and its spatial distribution is out-of-phase compared to the evanescent part of the E_x component. At the same time, the propagating part of the transmitted field (T_x) has no spatial variation linked to the film modulation since the tunneling through the film as a whole determines the transmission, the periodic modulation determines only the modes contributing to the tunneling process.

The near-field (NF) intensity distribution can be found in the following form:

$$|E_{\mathrm{NF}}|^2 = |c_z|^2 \sin^2(gx) + |b_x|^2 \cos^2(gx) + (T_x b_x^* + T_x^* b_x)\cos(gx) + |T_x|^2 \tag{26}$$

The last two terms in the above expression are relatively small due to the fact that $|T_x/b_x|^2 \ll 1$ confirming that the SPP field dominates the near-field intensity compared to the propagating field (Fig. 4). Moreover, the ratio $|c_z/b_z|^2 = g^2/\eta_{\mathrm{III}}^2 > 1$ shows that the most important contribution is from the first term in Eq. (26), related to the E_z component of the SPP field. For example, in the vicinity of the first transmission resonance $\lambda = 955$ nm (Fig. 2) this ratio is $|c_z/b_x|^2 \sim 10$. Thus, the spatial distribution of the near-field intensity along the x axis has minima in the points corresponding to both minima and maxima of the dielectric function $\varepsilon_{\mathrm{II}}(x)$, while the transmission maxima are shifted by a quarter of the grating period with respect to the minima of $\varepsilon_{\mathrm{II}}(x)$ (Fig. 5). If we consider the case of a hole array, the transmission in the near-field should have minima at the hole centers and middle of the metallic areas. The second term in Eq. (26) reduces the contrast of the observed distribution. This term corresponds to the field of the different polarization than that corresponding to the first term. Finally, the third term in Eq. (26) leads to the difference between the values of two adjacent intensity minima (above high and low dielectric constant areas), while the maxima have equal intensities. This picture is in complete agreement with the near-field distribution obtained with numerical modeling.[9–11]

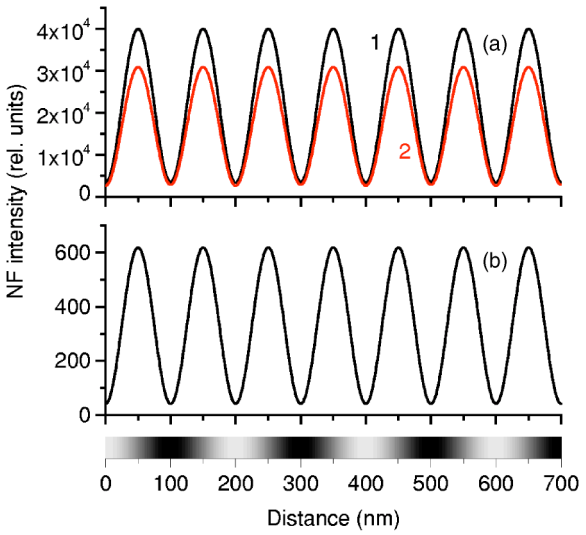

FIG. 5. (a) The near-field intensity above the surface ($z=-h-0$) at the wavelengths corresponding to (1) antisymmetric and (2) symmetric SPP modes. The parameters of the structure are the same as in Fig. 2(a). (b) The near-field intensity above the surface ($z=-h-0$) at the wavelength of the zero far-field transmission $t=0$ [Fig. 2(d)]. Grey-scale representation of the dielectric constant variation in the nanostructured film is also shown. The grey scale corresponds to the $\varepsilon_{\mathrm{II}}$ variations from –21 (black) to –31 (white). The NF intensity is normalized to the incident light intensity.

It should be noted that the far-field transmittance in the case of symmetrical surroundings is equal for both transmission resonances [Figs. 2(a) and 4(a)] while the near-field intensity is different [Figs. 4(c,d) and 5(a)]. The peak corresponding to symmetric SPP modes is smaller than the one related to antisymmetric SPP modes even in the lossless case considered here. This is probably related to the different field extension of these surface modes. The transmission due to the symmetric SPP mode will be further decreased if $Im\varepsilon_{\mathrm{II}} \neq 0$ is taken into account due to higher Ohmic losses associated with this mode.

For the structure under consideration, the transmitted field close to the surface is almost 200 times higher than the incident electromagnetic field, making almost 10^4 times intensity enhancement in the near-field. The increase of the modula-

tion depth ε_1 of the dielectric constant can lead to the increase of the contribution of the second term in Eq. (26) and more complex distribution of the near-field. Such a strong enhancement can be used for nanostructuring of the adjacent dielectric or implementation of nonlinear optical effects induced by the strong field close to a metal surface. It is obvious from Fig. 5 that in the minima of the near-field intensity distributions the longitudinal E_x component of the SPP field is dominant. The different contributions of various polarization components in the different places across the surface should be taken into account in interpretation of the near-field images of nanostructured metal surfaces since a probe tip of a scanning near-field microscope usually has different sensitivity for different polarizations of the detected light.

At the wavelength for which no far-field transmission is observed due to interaction of radiative and nonradiative SPP modes [Fig. 2(d)], the near-field intensity is strong indicating on the efficient excitation of the SPP modes which do not couple to photons [Fig. 5(b)]. The transmitted near-field intensity is more than two orders of magnitude higher than the intensity of the incident light. Polarization properties of the near-field are similar to the earlier discussed case of symmetrical surroundings. However, the spectral behavior of the different near-field components is different for this asymmetric structure (Fig. 6). In particular, the coefficient $(T_x b_x^* + T_x^* b_x)$ changes sign at the wavelength corresponding to the crossing of radiative and nonradiative branches of antisymmetric and symmetric film SPP Bloch modes. This is related to the π phase change of the b_x coefficient at the crossing wavelength. At the same time, the transmitted field T_x always changes the phase by π at the band gap edges.

It is interesting to note that according to Eq. (11), the condition on existence of a surface wave on a metal-substrate (medium III) interface is $\eta_{\mathrm{III}}^2 > 0$. Thus, for the incident light wavelength shorter than the critical wavelength $\lambda < \lambda_{\mathrm{cr}} = d\sqrt{\varepsilon_{\mathrm{III}}}$, additional bulk transmitted waves appear (Wood's anomaly). These waves propagate in medium III at the angles $\pm\theta_T$ to the surface normal defined by the expression $\sin\theta_T = \pm\lambda/\lambda_{\mathrm{cr}}$, thus the zero-order transmittance differs from the total transmittance of the nanostructure. The amplitudes of these waves resonantly increase in the vicinity of the SPP resonance on metal-(medium I) interface [the short-wavelength peak in Figs. 2(g,h)]. Similar waves can be observed in reflection from the structure at the angles $\sin\theta_R = \pm\lambda/d\sqrt{\varepsilon_{\mathrm{I}}}$. In the latter case, the resonant behavior of the reflected wave amplitude is determined by the higher branches of the SPP spectrum (in the case $\varepsilon_{\mathrm{I}} < \varepsilon_{\mathrm{III}}$).

III. CONCLUSION

We have analytically calculated the optical transmission and reflection coefficients of a periodically structured metal film capable of supporting surface plasmon polaritons. The developed theory allows the discrimination of the two transmission regimes related to symmetry and interaction between the SPP modes on the opposite film interfaces. These two regimes exhibit significantly different transmission spectra. The change of the transmission regime is determined by the crossing of the Bloch mode states related to the radiative SPP mode of the one interface and the nonradiative SPP mode of the other and depends on the modulation depth and the thickness of the film. At the crossing point, the transmission is suppressed. The influence of the adjacent media on the transmission spectra has also been studied. The exact knowledge of the electromagnetic mode structure of the system is used to analyse the near- and far-field properties of the transmitted light. Significant conversion of the transmitted light polarization is predicted in the near-field. The analytically calculated spectral dependencies are in a good agreement with the available experimental data and numerical simulations.

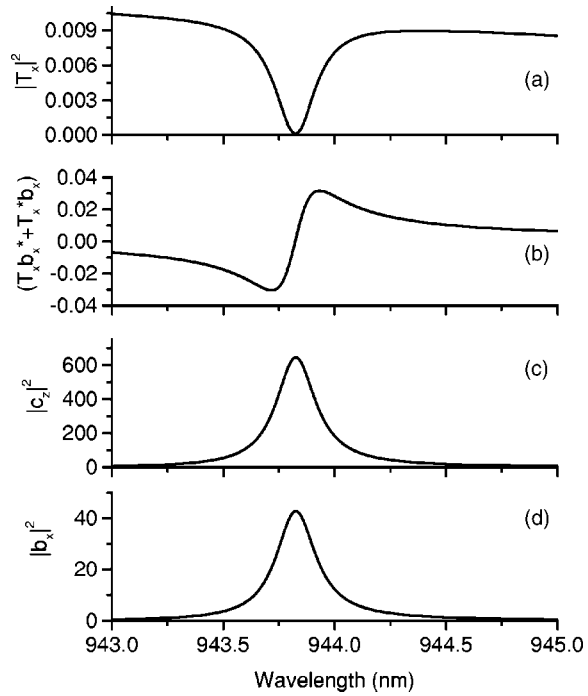

FIG. 6. Spectral dependencies of the coefficients in Eq. (26) determining the near-field intensity across the surface: (a) $|T_x|^2$, (b) $|T_x b_x^* + T_x^* b_x|$, (c) $|c_z|^2$, and (d) $|b_x|^2$. The parameters of the structure are the same as in Fig. 2(d).

ACKNOWLEDGMENTS

This work was supported in part by EPSRC. S.A.D. gratefully acknowledges the support from International Research Centre for Experimental Physics, The Queen's University of Belfast.

*Author to whom correspondence should be addressed. Email address: a.zayats@qub.ac.uk

[1] W. L. Barnes, A. Dereux, and T. W. Ebbesen, Nature (London) **424**, 824 (2003).
[2] A. V. Zayats and I. I. Smolyaninov, J. Opt. A, Pure Appl. Opt. **5**, S16 (2003).
[3] S. A. Darmanyan and A. V. Zayats, Phys. Rev. B **67**, 035424 (2003).
[4] A. M. Dykhne, A. K. Sarychev, and V. M. Shalaev, Phys. Rev. B **67**, 195402 (2003).
[5] I. I. Smolyaninov, A. V. Zayats, A. Stanishevsky, and C. C. Davis, Phys. Rev. B **66**, 205414 (2002).
[6] T. W. Ebbessen, J. Lezec, H. F. Ghaemi, T. Thio, and P. A. Wolff, Nature (London) **391**, 667 (1998).
[7] E. Popov, M. Nevière, S. Enoch, and R. Reinisch, Phys. Rev. B **62**, 16 100 (2000).
[8] L. Martin-Moreno, F. J. Garcia-Vidal, H. J. Lezec, K. M. Pellerin, T. Thio, J. B. Pendry, and T. W. Ebbesen, Phys. Rev. Lett. **86**, 1114 (2001).
[9] L. Salomon, F. Grillot, A. V. Zayats, and F. de Fornel, Phys. Rev. Lett. **86**, 1110 (2001).
[10] A. Krishnan, T. Thio, T. J. Kim, H. J. Lezec, T. W. Ebbesen, P. A. Wolf, J. Pendry, L. Martin-Moreno, and F. J. Garcia-Vidal, Opt. Commun. **200**, 1 (2001).
[11] D. Gérard, L. Salomon, F. de Fornel, and A. V. Zayats, Phys. Rev. B **69**, 113405 (2004).
[12] M. Nevière and E. Popov, *Light Propagation in Periodic Media* (Marcel Dekker, New York, 2003).
[13] *Surface Polaritons*, edited by V. M. Agranovich and D. L. Mills (North-Holland, Amsterdam, 1982).
[14] I. I. Smolyaninov, A. V. Zayats, A. Gungor, and C. C. Davis, Phys. Rev. Lett. **88**, 187402 (2002).
[15] D. Gérard, L. Salomon, F. de Fornel, and A. V. Zayats, Opt. Express **12**, 3652 (2004).